



Original scientific paper

Rice husk char as a potential electrode material for supercapacitors

Venkata Naga Kanaka Suresh Kumar Nersu^{1,✉}, Bhujanga Rao Annepu¹,
Satya Srinivasa Babu Patcha² and Subhakaran Singh Rajaputra³

¹Department of Instrument Technology, Andhra University College of Engineering (A),
Visakhapatnam, Andhra Pradesh 530003, India

²Center for Flexible Electronics, Department of Electronics and Communication Engineering, Koneru
Lakshmaiah Education Foundation, Vaddeswaram, AP, India

³Centre for Advanced Energy Studies, Koneru Lakshmaiah Education Foundation, Vaddeswaram, AP,
India

Corresponding author: ✉ sureshk834@gmail.com

Received: February 22, 2022; Accepted: March 28, 2022; Published: April 4, 2022

Abstract

Rice husk char (RHC), a carbon-based material, was obtained by thermal decomposition of rice husk (RH) biological waste. Physicochemical properties of RHC were determined using XRD, FTIR, FESEM, TGA, N₂ adsorption-desorption studies and contact angle measurement. A lab-scale supercapacitor (SC) was fabricated using as-prepared RHC and its supercapacitive behaviour was investigated using techniques like CV, GCD and EIS studies. Each of RHC electrode showed a specific capacitance of 80.2 F g⁻¹ at the constant charging/discharging current density of 0.05 A g⁻¹. RHC exhibited 90 % retention of its initial capacitance even after 5000 GCD. The presence of amorphous SiO₂ in RHC could contribute to the excellent wettability of RHC towards the water, enhancing its effective surface area by improving access of electrolyte ions into RHC. This remarkable supercapacitive performance of biological waste-derived RHC demonstrates its potential as a cost effective and environmentally benign electrode material for aqueous electrolyte-based SCs.

Keywords

Biochar; carbon-SiO₂ composite; superhydrophilicity; carbon cloth; nanocomposite gel polymer electrolyte; electric double layer capacitor (EDLC)

Introduction

Recently, an exponential increase in demand for the design and development of novel eco-friendly energy storage systems has been witnessed for harvesting energy from renewable resources [1]. Energy storage devices like supercapacitors (SCs) are well known for their high specific power, exceptional charge-discharge capability and long life [2]. Types of SCs include electric double-

layer capacitors (EDLCs), pseudocapacitors and hybrid SCs. EDLCs store charge in the electrochemical double layer (EDL) and are familiar for their prolonged cycle life and outstanding charge-discharge capabilities [3]. Activated carbon (AC), carbon black, graphene and carbon nanotubes (CNTs) are the most abundant electrode materials for EDLCs [4], and most of the commercially available EDLCs use AC as electrode material [5]. Recent advances in SC research were focused on exploring new resources for electrode materials that are economically feasible, abundant and derived from renewable precursors. Therefore, extensive research was directed toward deriving carbons from biological wastes for application as electrode materials in SCs [1].

Carbons derived from sugar cane bagasse [6], bamboo [7], straw of rice [8] and wheat [9], stems of sunflower [10] and lotus [11], stalks of corn [12] and cotton [13] were already applied in SCs as electrode materials. Natural fibers obtained from bamboo [14], jute [15] and hemp [16] and leaves of pine [17], lotus [18], *Ficus religiosa* [19] and eucalyptus [20] were also utilized to derive carbon-based electrode materials for SC application. Seed shells like coconut shells [21], macadamia nut shells [22] and oil palm kernel shells [23] were also used to derive carbons and tested as electrode materials in SCs.

Rice is the chief food source to around 50 % of the world population [24], and per annum, around 759.6 million tons of paddy is cultivated, while their de-husking results in around 150 million tons of rice husk (RH) [25]. RH disposal is a major concern to rice cultivators and millers [26], as burning or open dumping of RH pollutes the environment [27]. The main constituents of RH are cellulose, lignin, silica (SiO_2) and moisture [28,29]. De-silicized porous carbons obtained from RH through a two-step carbonization-activation method have been extensively applied as electrode materials in SCs [30]. Firstly, RH is carbonized and later, the carbonized RH is activated using activating agents like KOH [31], NaOH [32], H_3PO_4 [33] and ZnCl_2 [34], to obtain porous carbons. Few reported methods also include a pre-treatment step in which RH is leached using hydrogen fluoride (HF) before activation [35]. The use of such chemical agents consumes a major portion of the production cost and the release of chemical effluents causes harm to the environment, making these methods very expensive and not eco-friendly [36].

Removal of volatile components from RH results in carbon- SiO_2 composite, which can be applied in energy storage [37]. In the present work, rice husk char (RHC), a carbon- SiO_2 composite, was derived by thermal decomposition of RH without the steps like leaching and activation, making the process simple, cost-effective and eco-friendly. The RHC obtained is composed of amorphous SiO_2 and amorphous carbon. The physicochemical properties of RHC were investigated. A lab-scale symmetric SC was fabricated using RHC as electrode material, hydrothermally reduced carbon cloth (CCHy) as current collectors and graphene-based nanocomposite gel polymer electrolyte (NGPE). The supercapacitive behaviour of RHC in the full-cell configuration was evaluated using techniques like cyclic voltammetry (CV), galvanostatic charge-discharge (GCD) and electrochemical impedance spectroscopy (EIS) to determine the practicality of RHC as a potential biological waste derived carbon-based electrode material for SCs.

Experimental

Materials

RH was acquired from a local rice mill located in India and used directly for the preparation of RHC. Carbon cloth was obtained from AvCarb, USA. Propan-2-ol (Isopropanol / IPA), graphite powder (particle size $<20 \mu\text{m}$), sodium hydroxide (NaOH) pellets, ethanol 99.9 %, hydrogen peroxide (H_2O_2) (30 % w/v), polyvinylidene difluoride (PVDF) (homopolymer powder, M.W. $\sim 320,000$), N-methyl-2-pyrrolidone (NMP), sulphuric acid (H_2SO_4) 98 %, nitric acid (HNO_3), poly (vinyl alcohol)

(PVA) (M.W.~ 125,000), hydrochloric acid (HCl) 35–38 %, potassium permanganate (KMnO₄) and sodium nitrate (NaNO₃) were used as received. Whatman® qualitative filter paper: grade 1 (diam. 125 mm) procured locally was used as a separator in the fabricated lab-scale SC. Deionized (DI) water was employed in the entire work.

Preparation of RHC

RHC was obtained by thermal decomposition of RH (Figure 1). Untreated RH was placed in a silica crucible and covered with an aluminum foil. Small perforations were made to remove volatile compounds during the heating and minimize the reaction with oxygen. RH was heated up to 500 °C at a rate of 5 °C min⁻¹ to obtain black-colored charred flakes of RHC, which were later ground to obtain RHC powder.



Figure 1. Preparation of RHC through thermal decomposition of RH

Preparation of CCHy current collectors

Commercially obtained carbon cloth was modified to obtain CCHy following the synthesis procedure reported elsewhere [38]. Pieces of untreated carbon cloth were dropped into H₂SO₄ and HNO₃ (2:1) mixture. To this mixture, KMnO₄ (3 g) was added and stirred. Later, DI water (100 mL) was added and stirred continuously for three hours. To this mixture, H₂O₂ was added until the reaction turned transparent, resulting in chemically oxidized carbon cloths. The collected oxidized carbon cloths were rinsed several times, transferred into a DI water-filled PTFE lined autoclave, and heated at 180 °C for 14 h. Then CCHy were collected and dried under vacuum. The prepared CCHy were used as flexible current collectors while testing RHC as electrode material in full-cell studies.

Preparation of graphene-based NGPE

Hydrothermally reduced graphene oxide (HRG) was derived from graphene oxide (GO) following the synthesis procedure reported elsewhere [39]. GO was synthesized following modified Hummer's method from graphite precursor. Graphite (1 g) was dispersed in conc. H₂SO₄ (50 mL) into which NaNO₃ (1 g) was added and the suspension was placed in an ice bath and stirred for 4 h. Later, KMnO₄ (6 g) was added to the suspension and agitated for 48 h continuously. The suspension was kept in an ice bath followed by the addition of DI water (92 mL) and stirred for 2 h continuously. 30 % H₂O₂ (10 mL) was added to this suspension until the reaction turned yellow, resulting in GO. The GO suspension was centrifuged and the obtained precipitate was washed many times using 1 M HCl and DI water to gain a black-colored neutral GO suspension. Finally, to obtain GO, neutral GO suspension was centrifuged and filtered under vacuum to obtain a precipitate of GO, followed by

washing with ethanol, vacuum filtration and vacuum drying for 12 h at 70 °C. GO (0.1 g) was ground into fine powder and dispersed into DI water (100 mL) to obtain a dispersion of GO which pH was maintained at 11 using NaOH, and then transferred to a PTFE lined autoclave and heated for 14 h at 180 °C. Obtained HRG was vacuum dried (12 h at 60 °C) and ground to fine powder.

HRG (0.5 wt.%) incorporated sulfonated PVA (SPVA-HRG-0.5) hydrogel electrolyte was prepared by synthesis procedure reported elsewhere [40]. PVA (0.5 g) was added to a mixture of DI water (4 mL) and H₂SO₄ (270 µL) and stirred continuously for half an hour at 80 °C to obtain sulfonated PVA hydrogel (SPVA). 25 mg of HRG was suspended in IPA (10 mL) through ultrasonication and added slowly into SPVA hydrogel while stirring at 80 °C for 30 min in order to obtain SPVA-HRG-0.5. The as-prepared SPVA-HRG-0.5 was employed as an electrolyte while testing RHC as electrode material in full-cell studies.

Characterization studies

The structural properties and functional groups were investigated through X-ray diffraction (XRD) (Rigaku Miniflex 600) and Fourier-transform infrared (FTIR) spectroscopy (Cary 630) analyses, respectively. The surface morphology was determined from FESEM analysis (FEI-Quanta FEG 200F). Thermogravimetric analysis (TGA) was carried out under N₂ atmosphere up to 800 °C (20 °C min⁻¹ heating rate) using a thermal analyzer (STA 7200, Hitachi HTG) simultaneously. Surface area and porosity profile were established using surface area and porosity analyzer (Quantachrome NOVA 2200e). The wettability towards the water was determined from contact angle measurements (Kyowa DM-501). The electrochemical behaviour of RHC was evaluated in full-cell configuration using electrochemical workstation (PARSTAT PMC 2000A) by performing CV, GCD and EIS studies. An electrode ink, prepared by sonicating a mixture of RHC, MWCNTs and PVDF (80:10:10) in N-methyl-2-pyrrolidone (NMP) for 1 h, was drop cast over two CCHy (area of each CCHy = 0.8 cm²) and vacuum dried for 15 min at 120 °C to obtain flexible electrodes with RHC loading of 1 mg cm⁻². A full cell was fabricated by sandwiching SPVA-HRG-0.5 NGPE soaked Whatman® filter paper with flexible electrodes on either side.

Results and discussion

Physicochemical characterizations

Figure 2(a) represents X-ray diffractograms of RH and RHC powders. Both the RH and RHC diffractograms showed a characteristic broad peak of amorphous SiO₂ at 2θ value around 22° [41]. The broad diffraction peak observed at 2θ value of about 43° in both RH and RHC, indicates the presence of amorphous carbon [37].

Figure 2(b) represents the FTIR spectra of both RH and RHC. FTIR spectrum of RH shows a widespread band around 3284 cm⁻¹ resulting from stretching of O-H bonds of hydroxyl groups [42,43]. The small peaks observed around 2920 and 2852 cm⁻¹ in the spectra of RH resulted from C-H stretching of -CH₂ groups [44]. The thermal decomposition of RH to RHC has resulted in the removal of -OH and -CH₂ groups, indicated by the absence of their characteristic peaks in FTIR spectra of RHC. The peaks observed around 1717 and 1712 cm⁻¹ in RH and RHC, respectively, resulted from the stretching of carbonyl (C=O) groups [44]. The peaks observed around 1635 and 1634 cm⁻¹ in RH and RHC, respectively, resulted from C=C stretching [45]. The peaks observed around 1034 and 1078 cm⁻¹ in RH and RHC, respectively, are due to asymmetric stretching of Si-O-Si [46]. The peaks observed around 795 and 787 cm⁻¹ in RH and RHC, respectively, relate to symmetric stretching of Si-O-Si [46]. The intensities of bands related to SiO₂ in FTIR spectra of RHC were reduced compared to RH due to clenching and the development of a SiO₂ network on heating [44,47].

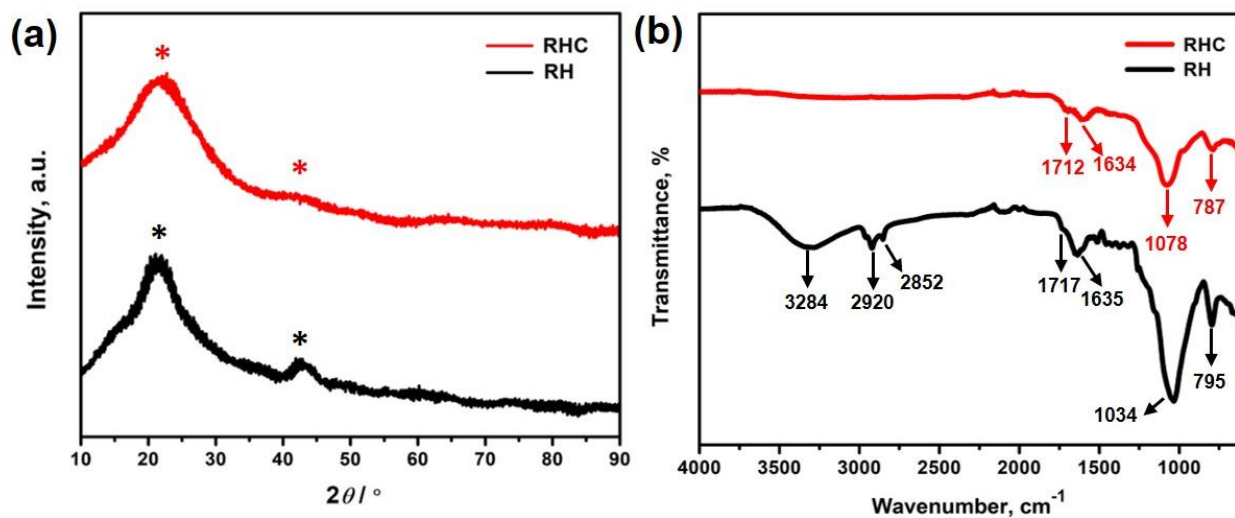


Figure 2. (a) X-ray diffractograms and (b) FTIR spectra of RH and RHC

Figure 3 represents FESEM images of RHC at different magnifications. Figures 3(a) and (b) depict the surface morphology of RHC composed of multiple irregular crevices, which could help in improving the surface area, thereby enhancing double layer (EDL) capacitance [48].

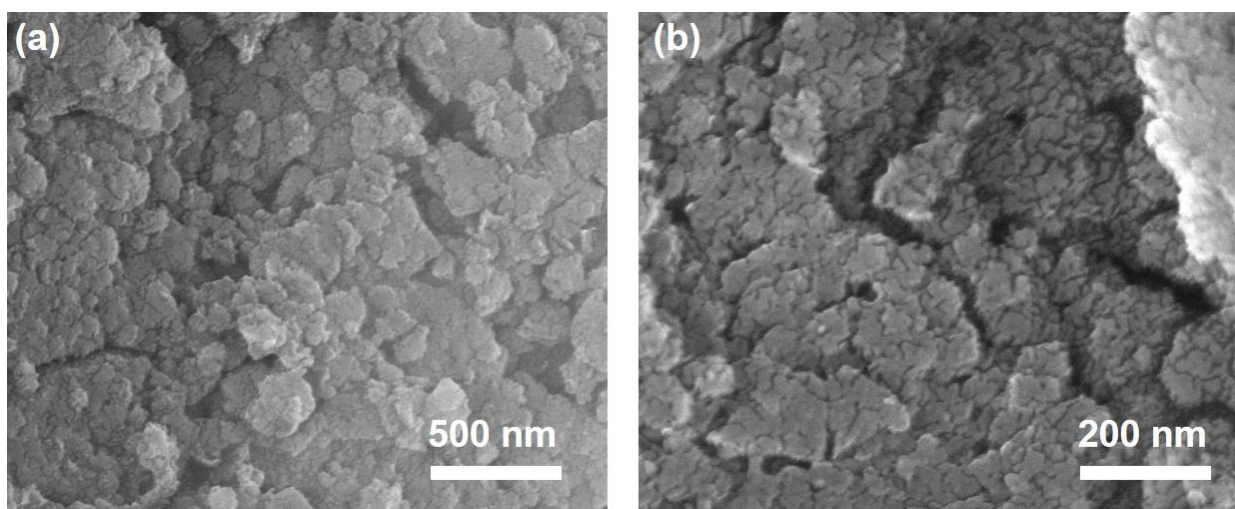


Figure 3. FESEM images depicting surface morphology of RHC at different magnifications

Figure 4 represents the TGA curve of RHC. In the TGA curve, RHC lost around 8 % of its weight below 100 °C due to the elimination of water content [49]. From 110 to 800 °C, a weight loss of 43 % was observed due to the breakdown of volatile compounds and the remaining 49 %, even after 800 °C, could be associated to amorphous SiO₂ [29]. From TGA, the wt.% of amorphous carbon and amorphous SiO₂ was determined to be around 43 and 49 %, respectively.

A pellet of 1.2 cm diameter was prepared using RHC powder and water contact angle measurement was performed by sessile drop technique. During contact angle measurement of RHC, the tested water droplet penetrated RHC resulting in a water contact angle of 0°, determining its superhydrophilic nature [50]. The superior wettability of RHC towards water could be attributed to hydrophilic metal oxide, *i.e.*, amorphous SiO₂ [51]. This superior wettability of RHC towards the water improves the access of SPVA-HRG-0.5 hydrogel electrolyte to deeper regions of RHC, thereby improving its supercapacitive behaviour by enhancing the EDL charging/discharging response [52]. The electrode-electrolyte interaction creates a considerable influence on charge-discharge ability, cycle life, charge storage and power delivery of a SC [53].

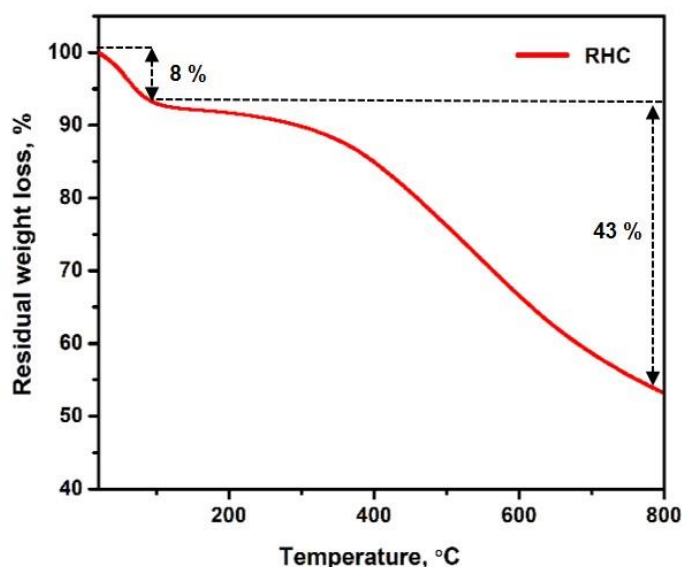


Figure 4. TGA curve of RHC

Figure 5(a) represents N_2 adsorption-desorption isotherm of RHC. The calculated Brunauer–Emmett–Teller (BET) surface area of RHC was around $38 \text{ m}^2 \text{ g}^{-1}$. Figure 5(b) represents the pore size distribution in RHC, where dV_0 and D represent differential pore volume and pore diameter, respectively. Figure 5(b) indicated that RHC mostly contains nanopores with an average pore size of around 2.8 nm. The presence of mesopores enhances capacitive retention in RHC by widening pathways for the transport of electrolyte ions [32].

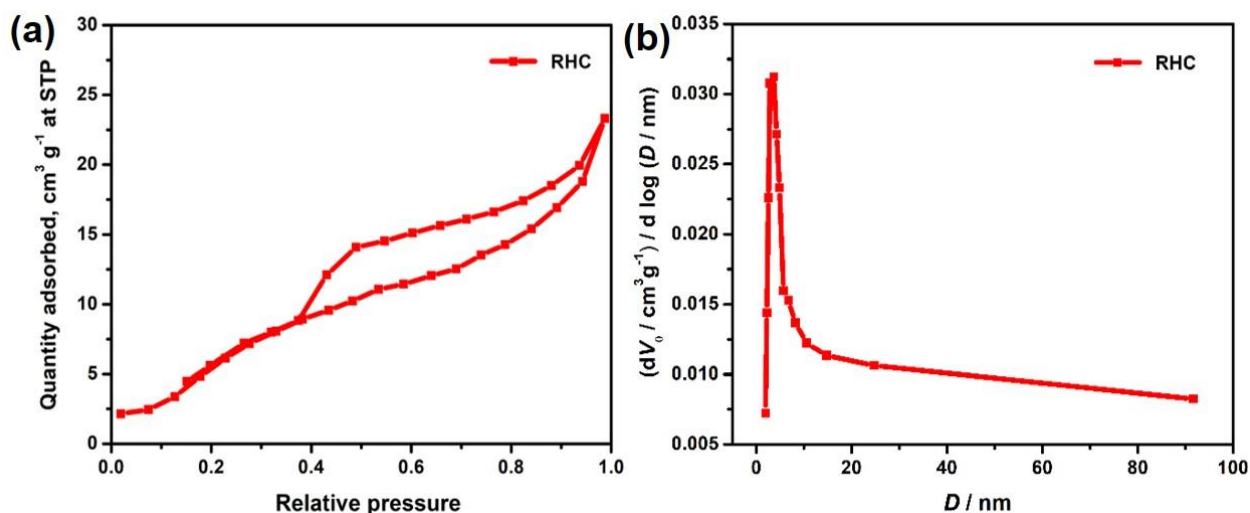


Figure 5. (a) N_2 adsorption-desorption isotherm and (b) pore size distribution in RHC

Electrochemical characterizations

Full-cell studies

The supercapacitive behaviour of RHC was evaluated in an in-house fabricated lab-scale full-cell. The electrochemical behavior was determined by performing CV, GCD and EIS studies.

CV was performed within a voltage window of 0 to 1 V at scan rates varying from 10 to 100 mV s^{-1} (Figure 6 (a)), which determined the excellent rate probability and reversibility of RHC [54]. GCD was performed within a potential window of 0 to 1 V at current densities ranging from 0.05 to 5 A g^{-1} (Fig. 6 (b)). The specific capacitance (C_s), specific energy (E_s), and specific power (P_s) of a single capacitor plate were calculated from GCD studies using equations 1, 2 and 3, respectively [55].

$$C_s = 2 \frac{I \Delta t}{m \Delta V} \quad (1)$$

$$E_s = \frac{C_s \Delta V^2}{8} \quad (2)$$

$$P_s = \frac{E_s}{\Delta t} \quad (3)$$

where, m , I , ΔV and Δt represent mass (g) of RHC (0.8 mg) on each electrode, constant discharge current (A), discharge voltage window (V), and discharge time (s), respectively.

RHC showed C_s in the range of 80.2 to 60 F g⁻¹ at constant current densities varying from 0.05 to 5 A g⁻¹, respectively. At 1 A g⁻¹ current density, RHC showed C_s of 66 F g⁻¹. RHC exhibited specific energy of 2.2 Wh kg⁻¹ at a specific power of 1 kW kg⁻¹. Figure 6(c) represents the Ragone plot obtained using calculated E_s and P_s values. Table 1 represents the experimental data obtained from GCD studies. Table 2 represents data for the comparison of supercapacitive performance of RHC with carbon-based electrode materials from RH precursors.

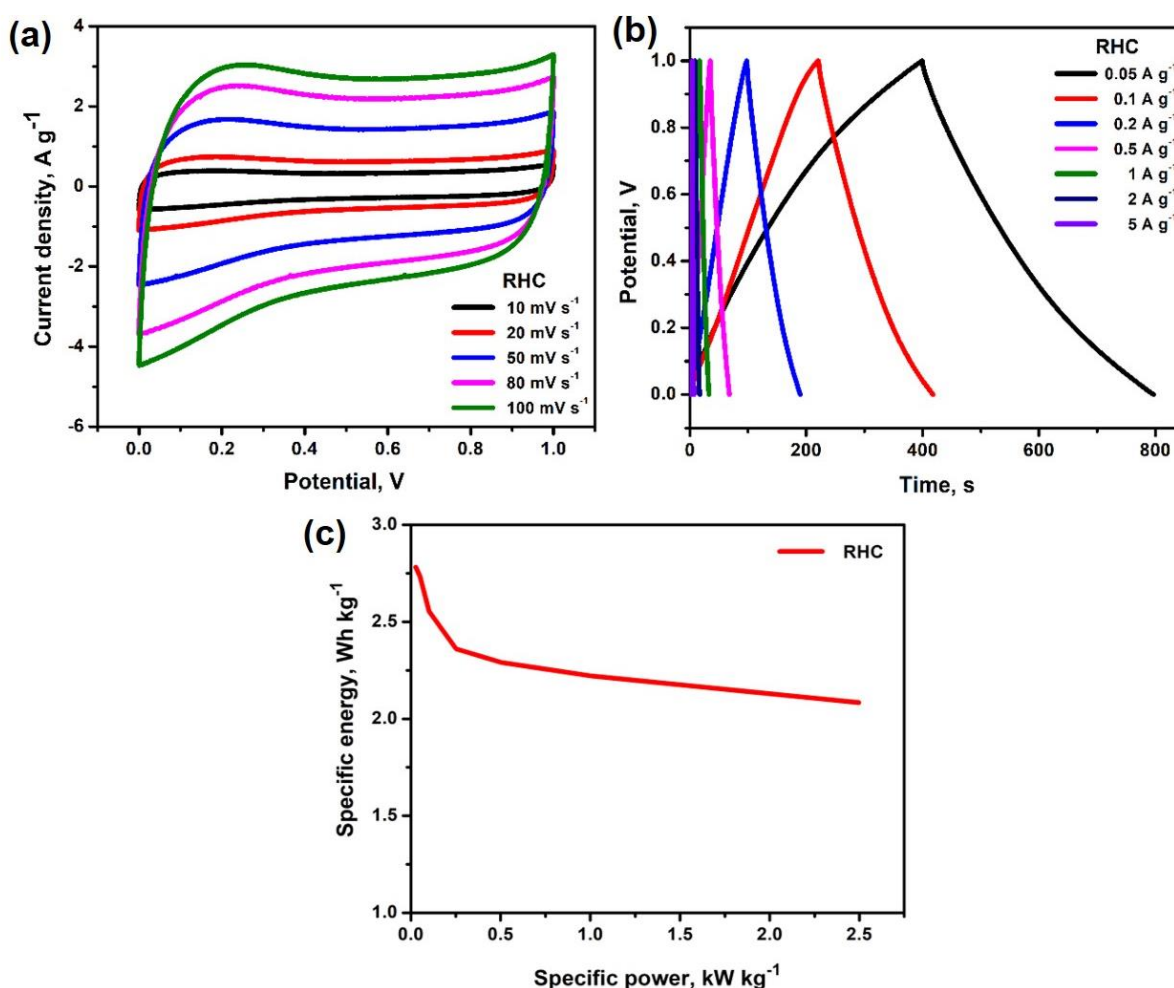


Figure 6. (a) CV curves of RHC at multiple scan rates, (b) GCD curves of RHC at various current densities and (c) Ragone plot of RHC

Cyclic stability of RHC-based flexible supercapacitor was tested for 5000 GCD cycles at a constant current density of 1 A g⁻¹. Figure 7(a) represents the CV curves of RHC at 50 mV s⁻¹, before and after cycling for 5000 GCD cycles. Figure 7(b) represents the GCD curves of RHC at 1 A g⁻¹, before and after cycling for 5000 GCD cycles. As shown in Figure 7(c), RHC retained 90 % of its initial capacitance during 5000 GCD cycles. EIS was performed within a frequency range of 100 kHz to 0.1 Hz at an amplitude of

5 mV at 0 V. Figure 7(d) represents the Nyquist plots obtained from EIS analysis of RHC before and after cycling for 5000 GCD cycles, showing a slight increase in cell impedance after cycling.

Table 1. Experimental data obtained from GCD studies of RHC electrodes in full-cell configuration

Current density, A g ⁻¹	IR drop, V	Discharge time, s	Specific capacitance, F g ⁻¹
0.05	0.01	401	80.2
0.1	0.017	197	78.8
0.2	0.032	92	73.6
0.5	0.071	34	68
1	0.111	16.5	66
2	0.218	8	64
5	0.592	3	60

Table 2. Comparison of specific capacitances of carbon-based electrode materials derived from RH precursor

Activating agent	Specific capacitance, F g ⁻¹	Electrolyte	Reference
NaOH	51.4 at 0.5 A g ⁻¹	6 M KOH	[32]
KOH	147 at 0.1 A g ⁻¹	6 M KOH	[56]
H ₃ PO ₄	112 at 1 A g ⁻¹	1 M Na ₂ SO ₄	[33]
NaOH	110.2 at 0.1 A g ⁻¹	6 M KOH	[36]
—	40.8 at 0.1 A g ⁻¹	6 M KOH	[36]
—	80.2 at 0.05 A g ⁻¹	SPVA-HRG-0.5	This work

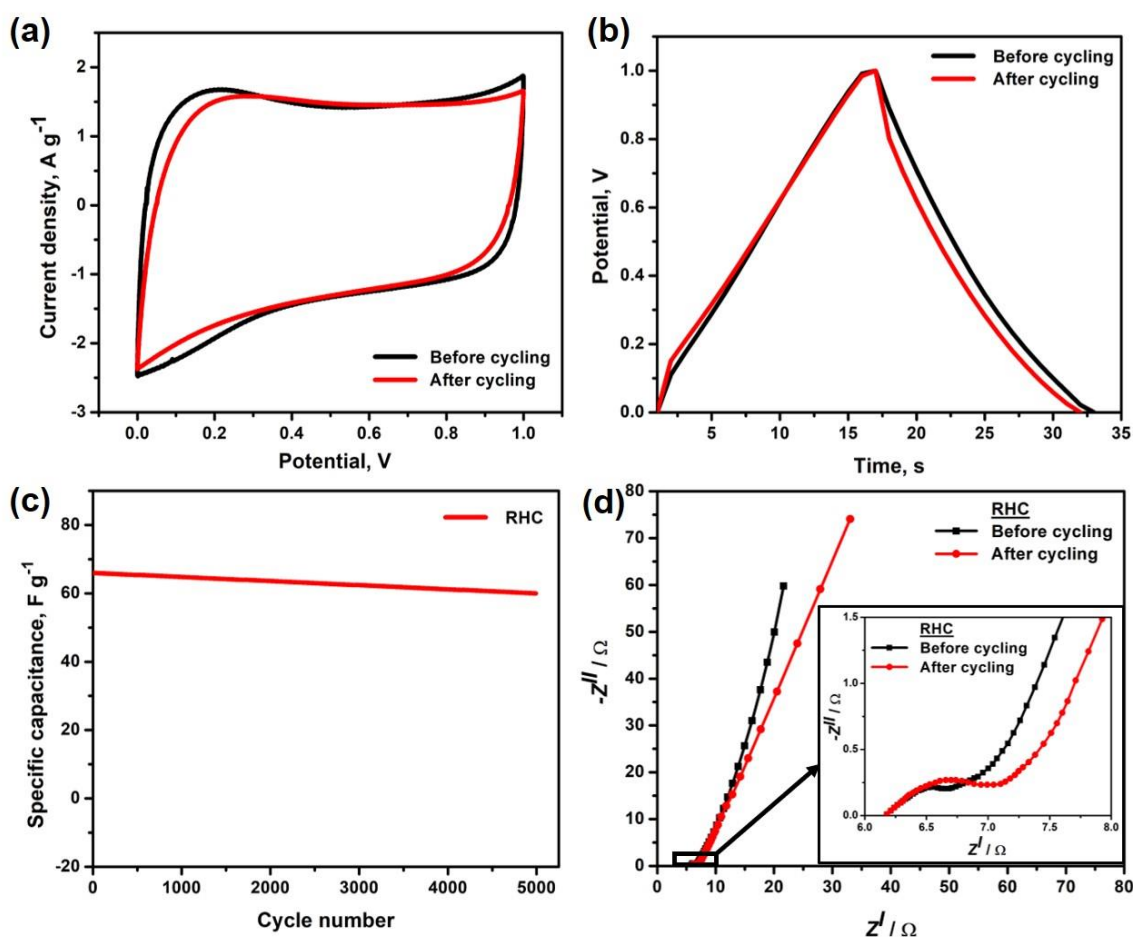


Figure 7. (a) CV curves of RHC at 50 mV s⁻¹ and (b) GCD curves of RHC at 1 A g⁻¹, respectively, before and after cycling; (c) cyclic stability of RHC for 5000 GCD cycles at 1 A g⁻¹ and (d) Nyquist plots of RHC before and after cycling; inset image shows the magnified image of Nyquist plots

Conclusions

RHC obtained through thermal decomposition of RH was characterized using physicochemical techniques. FESEM images confirmed the presence of crevices in RHC, which could enhance EDL formation by providing access of the electrolyte to the porous surface. XRD and FTIR analysis confirmed the presence of amorphous SiO₂ in RHC and the wt.% of SiO₂ and carbon in RHC were estimated to be around 49 and 43 %, respectively, from TGA analysis. BET specific surface area and average pore diameter of RHC were found to be around 38 m² g⁻¹ and 2.8 nm, respectively. The superior wettability of RHC towards the water, as confirmed from contact angle measurements, could be attributed to the presence of SiO₂. The practicality and applicability of RHC as potential electrode material in EDLCs were evaluated by fabricating a lab-scale SC and testing its supercapacitive performance using electrochemical techniques like CV, GCD and EIS. In full-cell (2-electrode) configuration, RHC at each electrode exhibited a specific capacitance of 80.2 F g⁻¹ at 0.05 A g⁻¹. Cyclic stability tests confirmed 90 % of capacitive retention in RHC even after 5000 GCD cycles at 1 A g⁻¹. The superior wettability of RHC, which in turn improved access of aqueous electrolyte ions into pores of RHC, thereby increasing the effective surface area of RHC, resulting in better supercapacitive behaviour. Current work emphasizes the potential of RHC as a biological waste derived carbon-based material as electrode material in aqueous electrolyte-based SCs.

Acknowledgments: *The authors are grateful to Er. Koneru Satyanarayana Garu, Hon'ble President, Koneru Lakshmaiah Education Foundation (Deemed to be University) for providing infrastructure to carry out this work. The authors thank Prof. Y. Anjaneyulu, Director, CAES, KLEF and Dr. K. Naga Mahesh, Nanosol Energy Pvt Ltd, Hyderabad for their support. The authors thank the MARC, BIT, Bengaluru for surface area and porosity measurement, the DST and the SAIF, IIT Madras, Chennai for FESEM observation, the CRF, CeNS, Bengaluru for contact angle measurement and the CoExAMMPC, VFSTR, Guntur, A. P. for XRD, TGA and FTIR measurements.*

References

- [1] S. Herou, P. Schlee, A. B. Jorge, M. Titirici, *Current Opinion in Green and Sustainable Chemistry* **9** (2018) 18-24. <https://doi.org/10.1016/j.cogsc.2017.10.005>
- [2] A. Afif, S. M. H. Rahman, A. T. Azad, J. Zaini, M. A. Islan, A. K. Azad, *Journal of Energy Storage* **25** (2019) 100852. <https://doi.org/10.1016/j.est.2019.100852>
- [3] T. Ramesh, N. Rajalakshmi, K. S. Dhathathreyan, L. Ram Gopal Reddy, *ACS Omega* **3** (2018) 12832-12840. <https://doi.org/10.1021/acsomega.8b01850>
- [4] G. Zhang, Y. Chen, Y. Chen, H. Guo, *Materials Research Bulletin* **102** (2018) 391-398. <https://doi.org/10.1016/j.materresbull.2018.03.006>
- [5] X. Chen, R. Paul, L. Dai, *National Science Review* **4(3)** (2017) 453-489. <https://doi.org/10.1093/nsr/nwx009>
- [6] H. Feng, H. Hu, H. Dong, Y. Xiao, Y. Cai, B. Lei, Y. Liu, M. Zheng, *Journal of Power Sources* **302** (2016) 164-173. <https://doi.org/10.1016/j.jpowsour.2015.10.063>
- [7] Y. Gong, D. Li, C. Luo, Q. Fu, C. Pan, *Green Chemistry* **19(17)** (2017) 4132-4140. <https://doi.org/10.1039/C7GC01681F>
- [8] S.-Y. Lu, M. Jin, Y. Zhang, Y.-B. Niu, J.-C. Gao, C. M. Li, *Advanced Energy Materials* **8(11)** (2018) 1702545. <https://doi.org/10.1002/aenm.201702545>
- [9] W. Liu, J. Mei, G. Liu, Q. Kou, T. Yi, S. Xiao, *ACS Sustainable Chemistry Engineering* **6(9)** (2018) 11595-11605. <https://doi.org/10.1021/acssuschemeng.8b01798>
- [10] Y. Wang, Z. Zhao, W. Song, Z. Wang, X. Wu, *Journal of Materials Science* **54(6)** (2019) 4917-4927. <https://doi.org/10.1007/s10853-018-03215-8>

- [11] Y. Zhang, S. Liu, X. Zheng, X. Wang, Y. Xu, H. Tang, F. Kang, Q.-H. Yang, J. Luo, *Advanced Functional Materials* **27(3)** (2017) 1604687. <https://doi.org/10.1002/adfm.201604687>
- [12] C. Wang, D. Wu, H. Wang, Z. Gao, F. Xu, K. Jiang, *Journal of Materials Chemistry A* **6(3)** (2018) 1244-1254. <https://doi.org/10.1039/C7TA07579K>
- [13] X. Tian, H. Ma, Z. Li, S. Yan, L. Ma, F. Yu, G. Wang, X. Guo, Y. Ma, C. Wong, *Journal of Power Sources* **359** (2017) 88-96. <https://doi.org/10.1016/j.jpowsour.2017.05.054>
- [14] L. Ji, B. Wang, Y. Yu, N. Wang, J. Zhao, *Electrochimica Acta* **331** (2020) 135348. <https://doi.org/10.1016/j.electacta.2019.135348>
- [15] C. Zequine, C.K. Ranaweera, Z. Wang, P. R. Dvornic, P. K. Kahol, S. Singh, P. Tripathi, O. N. Srivastava, S. Singh, B.K. Gupta, G. Gupta, R. K. Gupta, *Scientific Reports* **7(1)** (2017) 1174. <https://doi.org/10.1038/s41598-017-01319-w>
- [16] H. Wang, Z. Xu, A. Kohandehghan, Z. Li, K. Cui, X. Tan, T.J. Stephenson, C.K. King'ondo, C.M.B. Holt, B.C. Olsen, J.K. Tak, D. Harfield, A.O. Anyia, D. Mitlin, *ACS Nano* **7(6)** (2013) 5131-5141. <https://doi.org/10.1021/nn400731g>
- [17] G. Zhu, L. Ma, H. Lv, Y. Hu, T. Chen, R. Chen, J. Liang, X. Wang, Y. Wang, C. Yan, Z. Tie, Z. Jin, J. Liu, *Nanoscale* **9(3)** (2017) 1237-1243. <https://doi.org/10.1039/C6NR08139H>
- [18] S. Qu, J. Wan, C. Dai, T. Jin, F. Ma, *Journal of Alloys and Compounds* **751** (2018) 107-116. <https://doi.org/10.1016/j.jallcom.2018.04.123>
- [19] S.T. Senthilkumar, R. K. Selvan, *ChemElectroChem* **2(8)** (2015) 1111-1116. <https://doi.org/10.1002/celec.201500090>
- [20] A. K. Mondal, K. Kretschmer, Y. Zhao, H. Liu, C. Wang, B. Sun, G. Wang, *Chemistry-A European Journal* **23(15)** (2017) 3683-3690. <https://doi.org/10.1002/chem.201605019>
- [21] J. Xia, N. Zhang, S. Chong, D. Li, Y. Chen, C. Sun, *Green Chemistry* **20(3)** (2018) 694-700. <https://doi.org/10.1039/C7GC03426A>
- [22] X. Yan, Y. Jia, L. Zhuang, L. Zhang, K. Wang, X. Yao, *ChemElectroChem* **5(14)** (2018) 1874-1879. <https://doi.org/10.1002/celec.201800068>
- [23] I. I. Misnon, N. K. M. Zain, R. Abd Aziz, B. Vidyadharan, R. Jose, *Electrochimica Acta* **174** (2015) 78-86. <https://doi.org/10.1016/j.electacta.2015.05.163>
- [24] W. H. Kwan, Y. S. Wong, *Materials Science for Energy Technologies* **3** (2020) 501-507. <https://doi.org/10.1016/j.mset.2020.05.001>
- [25] M. López-Alonso, M. Martín-Morales, M. J. Martínez-Echevarría, F. Agrela, M. Zamorano, in: *Waste and by products in Cement-Based Materials, Innovative Sustainable Materials for a Circular Economy*, J. de Brito, C. Thomas, C. Medina, F. Agrela (Eds.), Woodhead Publishing, Cambridge, UK, 2021, p. 89-137. <https://doi.org/10.1016/B978-0-12-820549-5.00011-5>
- [26] S. G. Sara, *European Journal of Mechanical Engineering Research* **8(1)** (2021) 1-9. <https://www.eajournals.org/wp-content/uploads/A-Review-of-the-Potential-of-Rice-Husk-RH-and-Periwinkle-Shell-PWS.pdf>
- [27] N. Soltani, A. Bahrami, M. I. Pech-Canul, L. A. González, *Chemical Engineering Journal* **264** (2015) 899-935. <https://doi.org/10.1016/j.cej.2014.11.056>
- [28] B. Singh, in: *Waste and supplementary cementitious materials in concrete: characterisation, properties and applications*, R. Siddique, P. Cachim (Eds.), Woodhead Publishing, Cambridge, UK, 2018, p. 416-460. <https://doi.org/10.1016/B978-0-08-102156-9.00013-4>
- [29] S. K. S. Hossain, L. Mathur, P. K. Roy, *Journal of Asian Ceramic Societies* **6(4)** (2018) 299-313. <https://doi.org/10.1080/21870764.2018.1539210>
- [30] S. Zhang, Q. Zhang, S. Zhu, H. Zhang, X. Liu, *Energy Sources, Part A: Recovery, Utilization, and Environmental Effects* **43(3)** (2021) 282-290. <https://doi.org/10.1080/15567036.2019.1624881>

- [31] H. Wang, D. Wu, J. Zhou, H. Ma, D. Xu, B. Qian, S. Tao, Z. Wang, *BioResources* **13(2)** (2018) 4279-4289. https://ojs.cnr.ncsu.edu/index.php/BioRes/article/viewFile/BioRes_13_2_4279_Wang_Supercapacitor_Electrode/6076
- [32] Z. Chen, X. Wang, B. Xue, W. Li, Z. Ding, X. Yang, J. Qiu, Z. Wang, *Carbon* **161** (2020) 432-444. <https://doi.org/10.1016/j.carbon.2020.01.088>
- [33] A. Ganesan, R. Mukherjee, J. Raj, M. M. Shaijumon, *Journal of Porous Materials* **21(5)** (2014) 839-847. <https://doi.org/10.1007/s10934-014-9833-4>
- [34] X. He, P. Ling, M. Yu, X. Wang, X. Zhang, M. Zheng, *Electrochimica Acta* **105** (2013) 635-641. <https://doi.org/10.1016/j.electacta.2013.05.050>
- [35] Y. Xiao, M. Zheng, X. Chen, H. Feng, H. Dong, H. Hu, Y. Liang, S.P. Jiang, Y. Liu, *Chemistry Select* **2(22)** (2017) 6438-6445. <https://doi.org/10.1002/slct.201701275>
- [36] W. Zhang, N. Lin, D. Liu, J. Xu, J. Sha, J. Yin, X. Tan, H. Yang, H. Lu, H. Lin, *Energy* **128** (2017) 618-625. <https://doi.org/10.1016/j.energy.2017.04.065>
- [37] Y. Guo, X. Chen, W. Liu, X. Wang, Y. Feng, Y. Li, L. Ma, B. Di, Y. Tian, *Journal of Electronic Materials* **49(2)** (2020) 1081-1089 <https://doi.org/10.1007/s11664-019-07785-4>
- [38] S. Singh Rajaputra, P. Nagalakshmi, A. Yerramilli, K. Naga Makesh, *Journal of Electrochemical Energy Conversion and Storage* **18(4)** (2021) 041008. <https://doi.org/10.1115/1.4051143>
- [39] S. Singh Rajaputra, P. Nagalakshmi, A. Yerramilli, K. Naga Makesh, *Ionics* **27(9)** (2021) 4069-4082. <https://doi.org/10.1007/s11581-021-04144-4>
- [40] S. Singh Rajaputra, N. Pennada, A. Yerramilli, N. M. Kummara, *Journal of Electrochemical Science and Engineering* **11(3)** (2021) 197-207 <https://doi.org/10.5599/jese.1031>
- [41] M. K. Seliem, S. Komarneni, M. R. Abu Khadra, *Microporous and Mesoporous Materials* **224** (2016) 51-57. <https://doi.org/10.1016/j.micromeso.2015.11.011>
- [42] T. A. Tamanna, S. A. Belal, M. A. H. Shibly, A. N. Khan, *Scientific Reports* **11(1)** (2021) 7622. <https://doi.org/10.1038/s41598-021-87128-8>
- [43] Z. Emdadi, N. Asim, M. A. Yarmo, K. Sopian, *International Journal of Chemical Engineering and Applications* **6(4)** (2015) 273-276. <http://dx.doi.org/10.7763/IJCEA.2015.V6.495>
- [44] M. F. Zawrah, B. G. Alhogbi, *Ceramics International* **47(16)** (2021) 23240-23248. <https://doi.org/10.1016/j.ceramint.2021.05.036>
- [45] S. He, G. Chen, H. Xiao, G. Shi, C. Ruan, Y. Ma, H. Dai, B. Yuan, X. Chen, X. Yang, *Journal of Colloid and Interface Science* **582** (Part A) (2021) 90-101. <https://doi.org/10.1016/j.jcis.2020.08.021>
- [46] P. Araichimani, K. M. Prabu, G. S. Kumar, G. Karunakaran, S. Surendhiran, M. Shkir, *Research Square* (2021) 1-9. <https://doi.org/10.21203/rs.3.rs-1068714/v1>
- [47] P. Okoczuk, M. Łapiński, T. Miruszewski, P. Kupracz, L. Wicikowski, *Materials* **14(9)** (2021) 2158. <https://doi.org/10.3390/ma14092158>
- [48] T. Eguchi, D. Tashima, M. Fukuma, S. Kumagai, *Journal of Cleaner Production* **259** (2020) 120822. <https://doi.org/10.1016/j.jclepro.2020.120822>
- [49] N. F. T. Arifin, N. Yusof, N. A. H. Md Nordin, J. Jaafar, A. F. Ismail, F. Aziz, W. N. Wan Salleh, *International Journal of Hydrogen Energy* **46(60)** (2021) 31084-31095. <https://doi.org/10.1016/j.ijhydene.2021.02.051>
- [50] R. Asmatulu, W. S. Khan, R. J. Reddy, M. Ceylan, *Polymer Composites* **36(9)** (2015) 1565-1573. <https://doi.org/10.1002/pc.23063>
- [51] S. T. Gunday, E. Cevik, A. Yusuf, A. Bozkurt, *Journal of Physics and Chemistry of Solids* **137** (2020) 109209. <https://doi.org/10.1016/j.jpics.2019.109209>
- [52] H. Yang, Z. Bo, J. Yan, K. Cen, *International Journal of Heat and Mass Transfer* **133** (2019) 416-425. <https://doi.org/10.1016/j.ijheatmasstransfer.2018.12.134>

- [53] S. Alipoori, S. Mazinani, S. H. Aboutalebi, F. Sharif, *Journal of Energy Storage* **27** (2020) 101072. <https://doi.org/10.1016/j.est.2019.101072>
- [54] D. P. Dubal, N. R. Chodankar, D.-H. Kim, P.R. Gomez, *Chemical Society Reviews* **47** (2018) 2065-2129. <https://doi.org/10.1039/C7CS00505A>
- [55] H. Wang, H. Yi, X. Chen, X. Wang, *Journal of Materials Chemistry A* **2(9)** (2014) 3223-3230. <https://doi.org/10.1039/C3TA15046A>
- [56] E. Y. L. Teo, L. Muniandy, E.-P. Ng, F. Adam, A. R. Mohamed, R. Jose, K. F. Chong, *Electrochimica Acta* **192** (2016) 110-119. <https://doi.org/10.1016/j.electacta.2016.01.140>